

Self-consistent studies of the dipole response in neutron rich nuclei using realistic potentials

This content has been downloaded from IOPscience. Please scroll down to see the full text.

2015 J. Phys.: Conf. Ser. 580 012055

(<http://iopscience.iop.org/1742-6596/580/1/012055>)

View [the table of contents for this issue](#), or go to the [journal homepage](#) for more

Download details:

IP Address: 147.231.103.179

This content was downloaded on 23/02/2015 at 12:01

Please note that [terms and conditions apply](#).

Self-consistent studies of the dipole response in neutron rich nuclei using realistic potentials

F Knapp¹, N Lo Iudice^{2,3}, P Veselý⁴, F. Androzzi^{2,3}, G De Gregorio^{2,3}, A Porrino^{2,3}

¹ Faculty of Mathematics and Physics, Charles University in Prague, Czech Republic

² Dipartimento di Fisica, Università di Napoli Federico II, Napoli, Italy

³ Istituto Nazionale di Fisica Nucleare (INFN), Sezione di Napoli, Napoli, Italy

⁴ Institute of Nuclear Physics, Academy of Sciences of the Czech Republic, 250 68 Řež, Czech Republic

E-mail: frantisek.knapp@mff.cuni.cz

Abstract. The dipole response in neutron rich nuclei is investigated within self-consistent approaches which make direct use of a nucleon-nucleon optimized chiral potential complemented with a density dependent term simulating a three-body force. Hartree-Fock-Bogoliubov plus Tamm-Dancoff and random-phase approximations show that such a potential improves the description of the dipole modes with respect to other realistic interactions. The inclusion of the two-phonon states within an equation of motion method induces a pronounced fragmentation of both giant and pygmy resonances in agreement with recent experiments.

1. Introduction

Collective modes, and, more specifically, giant (GDR) and pygmy (PDR) dipole resonances in neutron rich nuclei are mostly investigated in phenomenological mean field approaches embedded within energy density functionals derived from Skyrme forces [1] or from relativistic meson-nucleon Lagrangians [2].

More recently, we have followed an alternative route proposed in [3], which consists in carrying out self-consistent calculations using directly realistic potentials derived from nucleon-nucleon (NN) forces, and adopted a V_{lowk} potential derived from the CD-Bonn NN interaction. Using such a potential, we have generated a Hartree-Fock-Bogoliubov (HFB) basis and, then, adopted both (quasi-particle) Tamm-Dancoff ((Q)TDA) and random-phase approximation ((Q)RPA) approaches to carry out a systematic study of the dipole response in several chains of neutron rich isotopes [4]. As in [3], however, we found necessary to add a corrective density dependent piece in order to get single-particle spectra sufficiently compressed so as to reproduce the main peak of the experimental GDR. Using such a modified Hamiltonian, we obtained spectra qualitatively consistent with experiments for all light, medium mass and heavy isotopes [4].

We have now performed analogous self-consistent (Q)TDA and (Q)RPA studies by making direct use of a recently determined chiral potential, dubbed NNLO_{opt}, with its parameters optimized so as to minimize the effects of the three-body forces [5]. This potential was adopted for ¹³²Sn in [6] and found to yield a much more compact single particle spectrum compared to V_{lowk} and, consequently, to produce a dipole strength distribution much closer to the region



of observation of the GDR peak. It was, nonetheless, still necessary to add the same density dependent term, though with a weaker coupling constant, in order to reproduce the centroid of the resonance. The potential, so modified, reproduces satisfactorily the gross features of both GDR and PDR. This is illustrated here for a chain of Ca isotopes.

(Q)TDA and (Q)RPA, however, were unable to describe the fine structure of the two resonances. So, we went beyond the mean field approximation and adopted the equation of motion phonon method (EMPM) [7–9] to study the dipole response within a space spanned by one plus two-phonon basis states [6]. The two phonons enhanced enormously the fragmentation of the dipole strength in both GDR a PDR regions, in better agreement with experiments. We report here also on the findings of such an investigation.

2. Brief outline of the EMPM method

The primary goal of the EMPM method is to generate a basis of n -phonon states $|n; \beta\rangle$ of energies E_β having the form

$$|n; \beta\rangle = \sum_{\lambda\alpha} C_{\lambda\alpha}^\beta \left\{ O_\lambda^\dagger \times |n-1, \alpha\rangle \right\}^\beta, \quad (1)$$

where the TDA particle-hole (p-h) phonon operator

$$O_\lambda^\dagger = \sum_{ph} c_{ph}^\lambda (a_p^\dagger \times b_h)^\lambda \quad (2)$$

of energy E_λ acts on the $(n-1)$ -phonon states $|n-1, \alpha\rangle$ of energies E_α . The procedure starts with the equations of motion

$$\langle n, \beta | [H, O_\lambda^\dagger] | n-1, \alpha \rangle = (E_\beta - E_\alpha) \langle n, \beta | O_\lambda^\dagger | n-1, \alpha \rangle. \quad (3)$$

We, then, expand the commutator and invert equation (2) in order to express the p-h operators, present in the expanded commutator, in terms of the phonon operators O_λ^\dagger . The outcome of this action is [9] the generalized eigenvalue equation

$$\sum_{\lambda'\alpha'\lambda_1\alpha_1} \left[\mathcal{A}^\beta(\lambda\alpha, \lambda_1\alpha_1) - E_\beta \delta_{\lambda_1\lambda} \delta_{\alpha_1\alpha} \right] \mathcal{D}^\beta(\lambda_1\alpha_1, \lambda'\alpha') C_{\lambda'\alpha'}^\beta = 0. \quad (4)$$

Here

$$\mathcal{D}^\beta(\lambda_1\alpha_1; \lambda'\alpha') = \left[\langle n-1, \alpha_1 | \times O_{\lambda_1} \right]_\beta \left[O_{\lambda'}^\dagger \times | n-1, \alpha' \rangle \right]_\beta \quad (5)$$

is the metric matrix and \mathcal{A}^β is a matrix of the simple structure

$$\mathcal{A}^\beta(\lambda\alpha, \lambda'\gamma) = (E_\lambda + E_\alpha) \delta_{\lambda\lambda'} \delta_{\alpha\gamma} + \sum_{\sigma} W(\beta\lambda'\alpha\sigma; \gamma\lambda) \mathcal{V}_{\lambda\alpha, \lambda'\gamma}^\sigma, \quad (6)$$

where W is a Racah coefficient and \mathcal{V}^σ a phonon-phonon potential given by

$$\mathcal{V}_{\lambda\alpha, \lambda'\gamma}^\sigma = \sum_{rstq} \rho_{\lambda\lambda'} ([q \times t]^\sigma) F_{qtrs}^\sigma \rho_{\alpha\gamma}^{(n)} ([r \times s]^\sigma). \quad (7)$$

We have denoted by $\rho_{\lambda\lambda'}$ and $\rho_{\alpha\alpha'}^{(n)}$, respectively, the $n=1$ (TDA) and the n -phonon ($n > 1$) density matrices

$$\rho_{\lambda\lambda'} ([r \times s]^\sigma) = \langle \lambda' | \left[a_r^\dagger \times b_s \right]^\sigma | \lambda \rangle \quad (8)$$

$$\rho_{\alpha\alpha'}^{(n)} ([r \times s]^\sigma) = \langle n; \alpha' | \left[a_r^\dagger \times b_s \right]^\sigma | n; \alpha \rangle. \quad (9)$$

The formal analogy between the structure of the phonon matrix $\mathcal{A}^\beta(\lambda\alpha, \lambda'\alpha')$ and the form of the TDA matrix $A^\lambda(ph; p'h')$ was pointed out [9]. The first is deduced from the second by replacing the TDA p-h energies with the sum of phonon energies ($E_\lambda + E_\alpha$) and the TDA p-h interaction with the phonon-phonon interaction \mathcal{V}^σ .

Equation (4) represents the eigenvalue equation in the overcomplete basis $\{O_\lambda^\dagger \times |n-1, \alpha\rangle\}^\beta$. The redundant states are eliminated by the procedure outlined in [7, 8], based on the Cholesky decomposition method.

Since recursive formulas hold for all quantities entering \mathcal{A} and \mathcal{D} , the eigenvalue equations are solved iteratively starting from the TDA phonons and, thereby, yield a set of orthonormal multiphonon states $\{|0\rangle, |1, \lambda\rangle, \dots |n, \alpha\rangle, \dots\}$.

In such a basis, the Hamiltonian matrix is composed of a sequence of diagonal blocks, one for each n , mutually coupled by off-diagonal terms $\langle n' | H | n \rangle$ which are non vanishing only for $n' = n \pm 1, n \pm 2$ and are computed by means of recursive formulas. A matrix of such a simple structure can be easily diagonalized yielding eigenfunctions of the form

$$|\Psi_\nu\rangle = \sum_{n\alpha} C_\alpha^{(\nu)} |n; \alpha\rangle. \quad (10)$$

3. Calculations and results

We adopted an intrinsic Hamiltonian obtained by subtracting the center of mass kinetic energy from the shell model kinetic operator and used the two-body potential

$$V_2 = NNLO_{opt} + V_\rho. \quad (11)$$

where $NNLO_{opt}$ is the NN chiral potential optimized so as to minimize the effects of the three-nucleon force [5], while V_ρ is a corrective repulsive, density dependent, two-body potential simulating a three-body contact force [10] which improves the description of bulk properties in closed shell nuclei [11] and yields more realistic single particle spectra and multipole nuclear responses [3, 4].

V_2 is adopted to generate a HFB basis in a configuration space which includes 13 harmonic oscillator major shells, up to the principal quantum number $N_{max} = 12$. Such a space is sufficient for reaching a good convergence. The self-consistent basis is used to compute the dipole strength distribution. We performed such a calculation in both (Q)TDA and (Q)RPA and found that the two approaches yield almost identical dipole spectra in all chains of isotopes [4, 6].

As illustrated in [6], the $NNLO_{opt}$ yields proton and neutron single particle spectra considerably more compressed than the ones produced by V_{lowk} derived from the CD-Bonn potential [4]. This compression is more consistent with experiments and improves the (Q)TDA and (Q)RPA descriptions of the dipole response. In ^{132}Sn , indeed, the peak of the strength distribution gets shifted from ~ 45 MeV, obtained when V_{lowk} is used, to ~ 23 MeV.

Such a strong shift, however, is not sufficient to reach the strongest experimental peak, observed at ~ 16 MeV. Hence the need of adding V_ρ , though with a weaker coupling constant. Such a potential pushes the dipole strength distribution in the region of observation as shown in figure 1 for a chain of Ca isotopes. Analogous results are obtained for O and Sn isotopes. (Q)RPA and (Q)TDA cross sections, computed by using a width $\Delta = 2.0$ MeV, follow closely the measured GDR cross sections. Such a good agreement is illustrated in the plots of figure 2 for ^{40}Ca and ^{48}Ca and holds for all the other nuclei.

Figure 1 shows that a peak appears around 10 MeV and becomes more and more pronounced as the excess neutrons increase. This trend, consistent with experiments, points toward the pygmy nature of these transitions, a suggestion supported by the analysis of the transition densities.

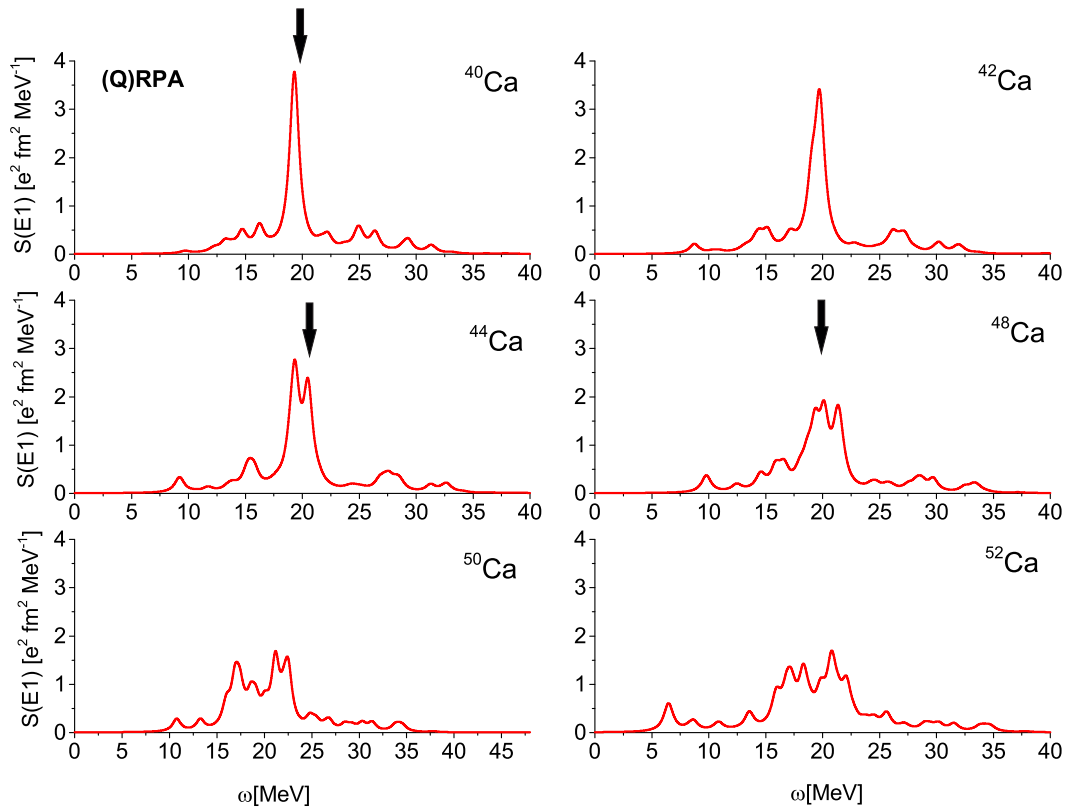


Figure 1. (Q)RPA $E1$ -strength distribution in a chain of Ca isotopes obtained using $NNLO_{opt} + V_{\rho}$.

Both (Q)TDA and (Q)RPA describe properly the gross features of GDR and PDR. To reproduce their fine structure it is necessary to go beyond the mean field approximation. This was done for ^{132}Sn by using the EMPM [6].

In the EMPM, the 1^- states are obtained by diagonalizing the Hamiltonian in a space spanned by one- ($|\lambda, 1^-\rangle$) plus two-phonon ($|(n=2)\beta, 1^-\rangle$) basis states. The latter states are generated in a subspace which includes the states $|(\lambda_1 \times \lambda_2)^{1-}\rangle \equiv \{O_{\lambda_1}^\dagger \times |\lambda_2\rangle\}^{1-}$ of energies $E_{\lambda_1} + E_{\lambda_2} \leq 30$ MeV,

The inclusion of the two-phonon states has a strong damping effect on the response. As shown in figure 3, compared to TDA, the EMPM cross section is severely quenched and reshaped due to the one- to two-phonon coupling. It has a smoother behavior and follows more closely the experimental points [12].

Both TDA and EMPM calculations yield a small peak in the cross section around ~ 10 MeV, fairly close in position and height to the one at ~ 9.8 MeV observed experimentally [12]. The EMPM strength collected by the low-lying states up to ~ 11 MeV exhausts $\sim 5.8\%$ of the TRK sum rule. This value is within the error of the measured fraction $4(3)\%$ [12].

The phonon coupling enhances greatly the fragmentation of the strength. This effect, partly hidden in the cross section due to the smoothing action of the Lorentzian, is clearly visible in the $E1$ spectra shown in [6]. As compared to TDA, the EMPM spectrum is much more dense and is composed of peaks of considerably shorter height in both GDR and PDR regions.

The low-lying spectrum is composed of a large number of levels excited by both isoscalar and isovector probes (figure 4), in analogy with the experimental spectrum produced by (γ, γ') and

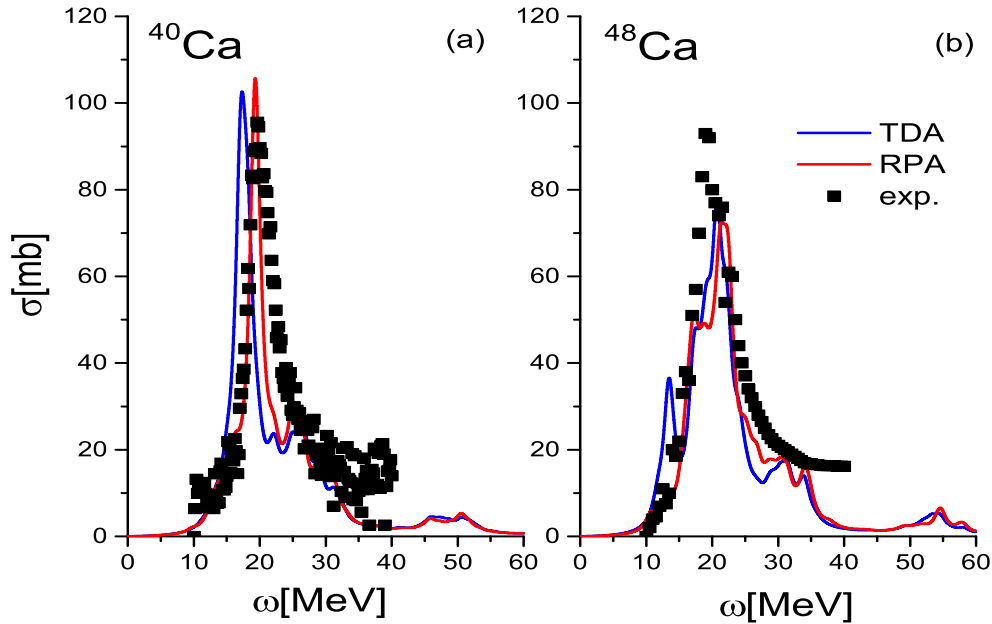


Figure 2. TDA and RPA versus experimental [17] cross sections in ^{40}Ca and ^{48}Ca

($\alpha, \alpha'\gamma$) experiments in the open shell ^{124}Sn [13–15]. Our calculation, however, does not predict for ^{132}Sn a splitting between isoscalar and isovector dipole modes at low-energy, at variance with the conclusions drawn from the analysis of the observed spectra in ^{124}Sn [16].

The mechanism of excitation suggests the pygmy nature of the low-lying states, a suggestion supported by the analysis of the wavefunctions and the transition densities [6].

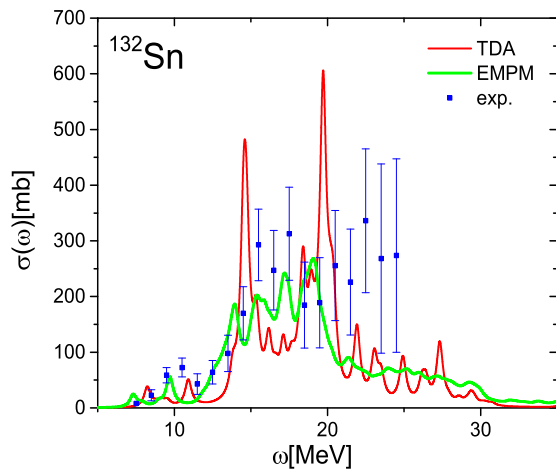


Figure 3. EMPM and TDA versus experimental cross sections in ^{132}Sn . A Lorentzian width $\Delta = 0.5$ MeV was used to compute the cross sections.

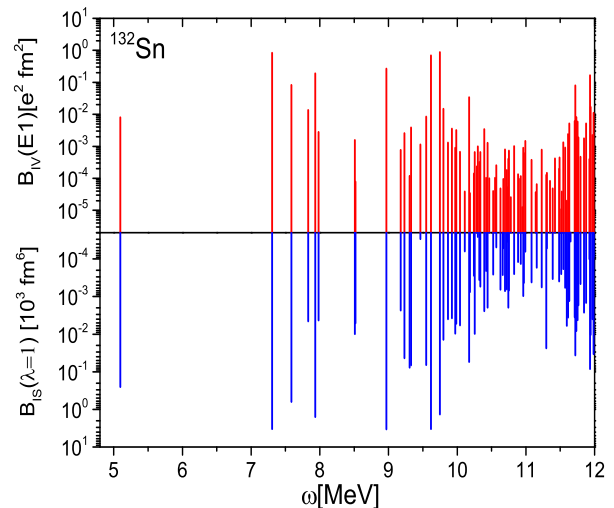


Figure 4. Low-lying isoscalar and isovector dipole transition strengths in ^{132}Sn

4. Conclusions

The first conclusion to be drawn from the above analysis is that the direct use of the optimized chiral potential $NNLO_{opt}$ yields much more realistic HF spectra compared to other realistic potentials and improves drastically the description of the dipole response. Such a potential, however, is not able to fill completely the gap between theory and experiments. This gap was filled here by adding a phenomenological density dependent repulsive term.

Another aspect to be pointed out is the high sensitivity of the response to the NN interaction. This property may be exploited to test different NN forces and to suggest a way of improving their parametrization.

Last but not least, the present study has pointed out the crucial role of complex configurations, two-phonon states in our case, in damping the GDR and in enhancing the density of low-lying levels as recent experiments require.

Acknowledgments

This work was partially supported by the Czech Science Foundation (Project No. P203-13-07117S)

References

- [1] Bender M, Heenen P H and Reinhard P G 2003 *Rev. Mod. Phys.* **75** 121
- [2] Vretenar D, Afanasjev A V, Lalazissis G A and Ring P 2005 *Phys. Rep.* **409** 101
- [3] Hergert H, Papakonstantinou P and Roth R 2011 *Phys. Rev. C* **83**(6) 064317
- [4] Bianco D, Knapp F, Lo Iudice N, Veselý P, Andreozzi F, De Gregorio G and Porrino A 2014 *Journal of Physics G: Nuclear and Particle Physics* **41** 025109
- [5] Ekström A, Baardsen G, Forssén C, Hagen G, Hjorth-Jensen M, Jansen G R, Machleidt R, Nazarewicz W, Papenbrock T, Sarich J and Wild S M 2013 *Phys. Rev. Lett.* **110**(19) 192502
- [6] Knapp F, Lo Iudice N, Vesely P, Andreozzi F, De Gregorio G and Porrino A 2014 *Phys. Rev. C* **90** 014310
- [7] Andreozzi F, Knapp F, Lo Iudice N, Porrino A and Kvasil J 2007 *Phys. Rev. C* **75**(4) 044312
- [8] Andreozzi F, Knapp F, Lo Iudice N, Porrino A and Kvasil J 2008 *Phys. Rev. C* **78**(5) 054308
- [9] Bianco D, Knapp F, Lo Iudice N, Andreozzi F and Porrino A 2012 *Phys. Rev. C* **85**(1) 014313
- [10] Waroquier M, Heyde K and Vincx H 1976 *Phys. Rev. C* **13**(4) 1664–1673
- [11] Günther A, Roth R, Hergert H and Reinhardt S 2010 *Phys. Rev. C* **82**(2) 024319
- [12] Adrich P, Klimkiewicz A, Fallot M, Boretzky K, Aumann T, Cortina-Gil D, Pramanik U D, Elze T W, Emling H, Geissel H, Hellström M, Jones K L, Kratz J V, Kulesa R, Leifels Y, Nociforo C, Palit R, Simon H, Surówka G, Sümmerer K and Waluś W (LAND-FRS Collaboration) 2005 *Phys. Rev. Lett.* **95**(13) 132501
- [13] Govaert K, Bauwens F, Bryssinck J, De Frenne D, Jacobs E, Mondelaers W, Govor L and Ponomarev V Y 1998 *Phys. Rev. C* **57**(5) 2229–2249
- [14] Endres J, Litvinova E, Savran D, Butler P A, Harakeh M N, Harissopulos S, Herzberg R D, Krücken R, Lagoyannis A, Pietralla N, Ponomarev V Y, Popescu L, Ring P, Scheck M, Sonnabend K, Stoica V I, Wörtche H J and Zilges A 2010 *Phys. Rev. Lett.* **105**(21) 212503
- [15] Endres J, Savran D, Butler P A, Harakeh M N, Harissopulos S, Herzberg R D, Krücken R, Lagoyannis A, Litvinova E, Pietralla N, Ponomarev V, Popescu L, Ring P, Scheck M, Schlüter F, Sonnabend K, Stoica V I, Wörtche H J and Zilges A 2012 *Phys. Rev. C* **85**(6) 064331
- [16] Savran D, Babilon M, van den Berg A M, Harakeh M N, Hasper J, Matic A, Wörtche H J and Zilges A 2006 *Phys. Rev. Lett.* **97**(17) 172502
- [17] Erokhova V A, Elkin M A, Izotova A V, Ishkhanov B S, Kapitonov I M, Lileeva E I and Shirokov E V 2003 *Izv. Rossiiskoi Akademii Nauk, Ser.Fiz.* **67** 1479 (EXFOR M0653.002 and M0653.005)